



Accepted Article

Title: Coordination-Assembled Lanthanide-Organic Ln_3L_3 Sandwiches or Ln_4L_4 Tetrahedron: Structural Transformation and Luminescence Modulation

Authors: Shao-Jun Hu, Xiao-Qing Guo, Li-Peng Zhou, Li-Xuan Cai, and Qing-Fu Sun*

This manuscript has been accepted and appears as an Accepted Article online.

This work may now be cited as: *Chin. J. Chem.* **2019**, *37*, 10.1002/cjoc.201900101.

The final Version of Record (VoR) of it with formal page numbers will soon be published online in Early View: <http://dx.doi.org/10.1002/cjoc.201900101>.

Coordination-Assembled Lanthanide-Organic Ln₃L₃ Sandwiches or Ln₄L₄ Tetrahedron: Structural Transformation and Luminescence Modulation

Shao-Jun Hu,^{ab} Xiao-Qing Guo,^{ac} Li-Peng Zhou,^a Li-Xuan Cai,^a and Qing-Fu Sun^{*,a,b,c}

^a State Key Laboratory of Structural Chemistry, Fujian Institute of Research on the Structure of Matter, Chinese Academy of Sciences, Fuzhou 350002, PR China

^b College of Chemistry, Fuzhou University, Fuzhou 350108, PR China

^c University of Chinese Academy of Sciences, Beijing 100049, PR China

Cite this paper: *Chin. J. Chem.* 2019, 37, XXX–XXX. DOI: 10.1002/cjoc.201900XXX

Photo-functional supramolecular lanthanides assemblies have shown great potential in the materials and biomedical fields. Two new tri(tridentate) ligands (**L3** and **L4**) highlighting small variation of the connection position to the central tridentate linkers have been designed, which leads to the emergent formation of either Ln₃L₃-type sandwich structures or Ln₄L₄-type tetrahedral cages. Moreover, nonlinear enhancement of lanthanide luminescence based on the modulation of inter-ligand charge-transfer states has been revealed on the mix-ligand Ln₃L₃ sandwiches. Our results provide important guidance for structure-design and photoluminescence optimization of supramolecular lanthanide-organic assemblies.

Background and Originality Content

Coordination-assembled discrete supramolecular architectures show many promising applications, such as biomimetic catalysis,^[1] molecular sensing,^[2] ion extraction,^[3] bio-imaging and cancer therapy.^[4] In contrast with the intense reports on metallosupramolecular edifices constructed with transition metals,^[5] multi-nuclear lanthanide-organic architectures are far less studied.^[6] Due to their particular optical, electric and magnetic characteristics, mononuclear clathrates, bundles or dinuclear helicates of lanthanides have shown great potential in the materials and biomedical fields.^[7] However, high-nuclear and sophisticated lanthanide-organic assemblies are still rare because of the challenges in taming the intrinsic liability and flexibility on lanthanide coordination.^[8]

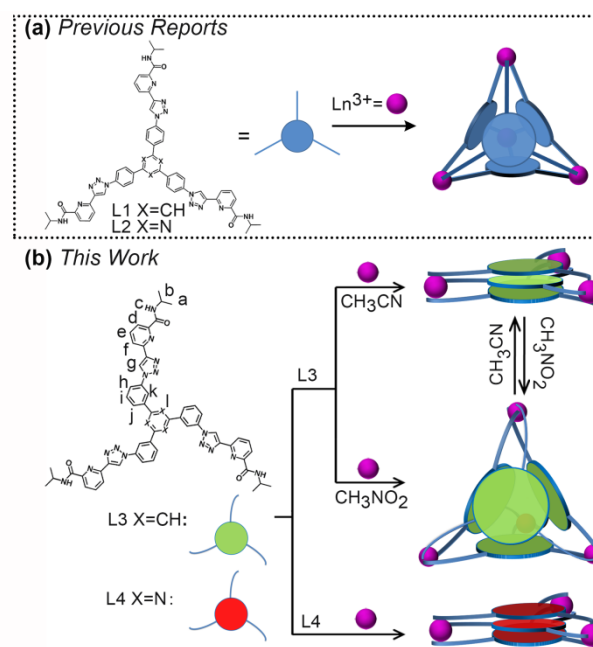
Supramolecular transformation is an efficient method for the generation and functionalization of discrete supramolecular assemblies.^[9] In-depth understanding of supramolecular transformation helps not only in mimicking the biological transformation processes but also in the design of smart functional materials. So far, stimuli-responsive supramolecular transformations triggered by solvent,^[10] concentration,^[11] pH,^[12] light,^[13] metal/ligand ratio,^[14] guests,^[15] and so on have been accomplished. Recently, our group has reported a systematic structure evolution of the chiral lanthanide coordination edifices from helicates and tetrahedrons to cubes via subtle ligand variations and concentration effect.^[2a, 6a]

Due to the Laporte symmetry-forbidden 4f-4f transitions on lanthanides (with molar absorption coefficient $\epsilon < 10^2 \text{ M}^{-1} \text{ cm}^{-1}$),^[16] “antenna” sensitization of lanthanide luminescence through the adjacent organic chromophores is necessary.^[17] To obtain bright luminescent lanthanide complexes, most efforts have been focused on designing appropriate ligands with proper energy gap between the excited state of the donor ligands (usually the triplet state T1) and the accepting emitting states of the lanthanides.^[18]

Recently, we found that ligands based on triazole-pyridine-amido (tpa) chelation arms (**L1** and **L2**) could form bright luminescent lanthanide-organic polyhedra.^[19] Herein, two new tpa-based tri(tridentate) ligands (**L3** and **L4**) highlighting small variation of the connection position to the central tridentate linkers have been designed, which leads to the emergent formation of new Ln₃L₃-type sandwich structures or Ln₄L₄-type tetrahedral cage (Scheme 1). Transformation between Ln₃L₃ and Ln₄L₄ has also

been realized by switching the solvents with different polarity. Moreover, non-linear luminescent enhancement through an inter-ligand charge transfer sensitization mechanism has been revealed during the mixed-ligand self-assembly of the Ln₃L₃ sandwiches.

Scheme 1 Coordination-directed self-assembly and structural transformation of Lanthanide-organic Ln₃L₃ sandwiches and Ln₄L₄ Tetrahedron.



Results and Discussion

Ligand design and synthesis. Based on geometrical principle, *C*₃-symmetry tris-(tridentate) ligands combined with nine-coordinating *C*₃-symmetry Lanthanide nodes usually form M₄L₄-type tetrahedron.^[2c, 3, 19-20] Indeed, full-conjugated ligands with triphenyl-benzene or triphenyl-triazine cores decorated by the triazole-pyridine-amido (tpa) chelating arms are known to self-assemble with Ln³⁺ (Ln = Eu, Tb, Sm, Dy) to form bright luminescent Ln₄L₄ tetrahedra.^[19] Meanwhile, we also disclosed that the offset arrangement of the chelating groups in the

*E-mail: qfsun@fjirsm.ac.cn

This article has been accepted for publication and undergone full peer review but has not been through the copyediting, typesetting, pagination and proofreading process, which may lead to differences between this version and the Version of Record. Please cite this article as doi: 10.1002/cjoc.201900101

bis-(bidentate) ligands can dictate the final outcomes of the assembly, where $\text{Ln}_{2n}\text{L}_{3n}$ ($n = 1, 2, 4$) could be selectively obtained.^[21] This finding persuaded us to check whether the variation of the connection angles between chelation arm and the central tridentate spacer has influence on the final product. Bear this in mind, two new tris-(tridentate) ligands, **L3** and **L4**, where the connection angle between the chelating arms and the spacer is changed from 180 to 120 degrees (Scheme 1) have been designed. Both ligands were synthesized by previously reported method,^[19] which have been fully characterized by NMR and high-resolution ESI-MS spectroscopy. (See experimental section for details.) Surprisingly, **L3** and **L4** both tend to form Ln_3L_3 sandwich structures instead of Ln_4L_4 tetrahedron when self-assemble with Ln^{3+} . To the best of our knowledge, this is the first example of lanthanide supramolecular sandwich architecture. Moreover, ligand **L3** can also self-assemble with Ln^{3+} to form the known Ln_4L_4 tetrahedron, where solvent-triggered transformation between Ln_3L_3 and Ln_4L_4 took place.

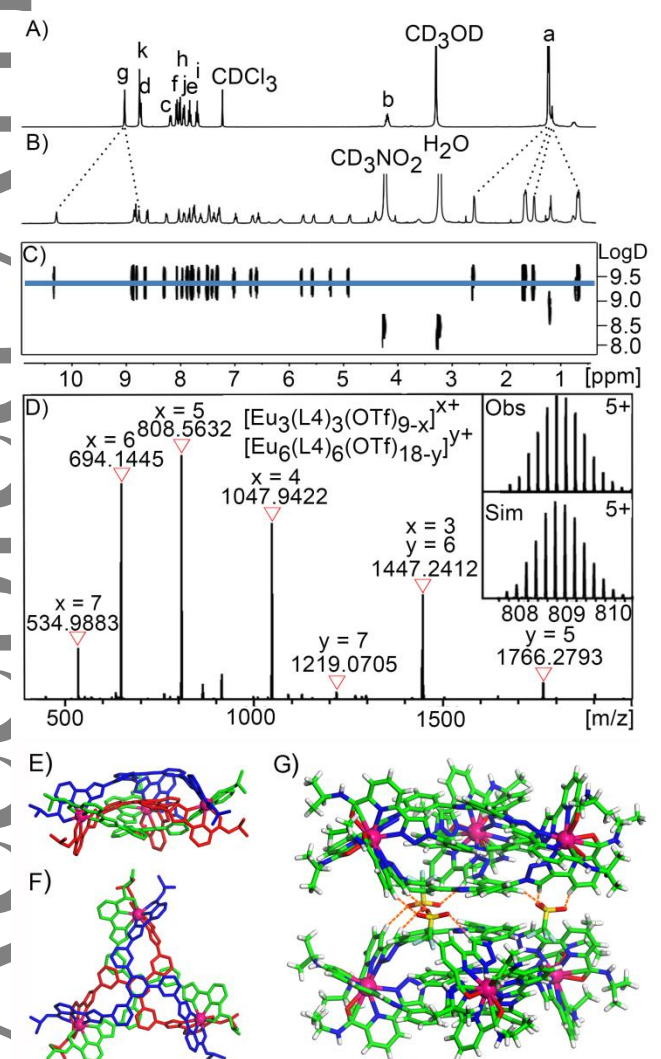


Figure 1 Characterization of the self-assembly of **L4** with $\text{Eu}(\text{OTf})_3$: ^1H NMR (400 MHz, 293 K) spectra of (A) free ligand **L4** (in $\text{CDCl}_3/\text{CD}_3\text{OD} = 4:1$) and (B) the $\text{Eu}_3(\text{L4})_3(\text{OTf})_9$ complex (in $\text{CD}_3\text{NO}_2/\text{CD}_3\text{OD}=4:1$); (C) ^1H DOSY and (D) ESI-TOF-MS spectra of the $\text{Eu}_3(\text{L4})_3(\text{OTf})_{12}$ complex with insets showing the observed (Obs) and simulated (Sim) isotopic patterns of the peaks corresponding to $[\text{Eu}_3(\text{L4})_3(\text{OTf})_4]^{5+}$. X-ray crystal structure of the $\text{Eu}_3(\text{L4})_3$ complex: Side view (E) and top view (F) of the discrete $\text{Eu}_3(\text{L4})_3$ assembly; (G) $(\text{OTf})_3@[\text{Eu}_3(\text{L4})_3]_2$ dimeric structure refined in the asymmetric unit (Color mode: Eu, purple sphere; C, green; N, dark blue; O, red; F, gray-green; S, yellow).

Complex of $\text{Eu}_3(\text{L4})_3(\text{OTf})_9$. When equimolar amount of $\text{Eu}(\text{OTf})_3$ and **L4** were added into a mixed solvent of deuterated acetonitrile and methanol (v/v, 4:1) and stirred at 50 °C for 1 hour, the turbid suspension gradually turned into a homogeneous solution. ^1H NMR indicated quantitative formation of a single product with low symmetry, as roughly two sets of ligand signals in a 1:2 ratio are observed, except for the further splitting of the isopropyl groups (Figure 1A, B). Compared with the free ligand, most signals arising from the assembly are shifted, which can be attributed to paramagnetic Eu^{III} centers. All signals can be fully assigned with the help of ^1H - ^1H COSY spectra (Figure S12). Diffusion-ordered ^1H NMR (DOSY) also indicated the formation of a single species in solution, with one diffusion band observed at a diffusion coefficient of $D = 3.55 \times 10^{-10} \text{ m}^2\text{s}^{-1}$ (Figure 1C). High-resolution ESI-TOF-MS clearly confirmed the formation of the trinuclear supramolecular architecture with a formula of $\text{Eu}_3(\text{L4})_3(\text{OTf})_9$ (Figure 1D). A series of peaks with $m/z = 810.1722$, 1049.9542, 1449.5897 consistent with the successive loss of OTf^- counter ions on $\text{Eu}_3(\text{L4})_3(\text{OTf})_9$ are observed, which can be further verified by comparing to the isotopic patterns. For example, the simulated isotopic pattern for $[\text{Eu}_3(\text{L4})_3(\text{OTf})_5]^{4+}$ shown in the insets of Figure 1D perfectly match the experimentally observed one.

The structure of $\text{Eu}_3(\text{L4})_3(\text{OTf})_9$ was ultimately confirmed by X-ray diffraction analysis. Single crystals were obtained by slow vapor diffusion of chloroform into the acetonitrile solution of $\text{Eu}_3(\text{L4})_3(\text{OTf})_9$ after weeks. It has to be pointed out this crystal diffracts very weakly in nature due to a giant “void” of $25,577 \text{ \AA}^3$ (roughly 64.7% of unit cell volume), where highly disordered charge-balancing counter ions and solvent molecules have been masked by a Platon/SQUEEZE routine.^[22] As shown in Figure 1E, the discrete $\text{Eu}_3(\text{L4})_3$ assembly displays a triple-decker sandwich structure, where three Eu vertices define a pseudo-regular triangle with an average $\text{Eu}\cdots\text{Eu}$ distance measured to be 15.6 Å. All Eu centers are nine-coordinated with mechanical-coupled cooperative $\Delta\Delta\Delta$ or $\Lambda\Lambda\Lambda$ configurations, resulting in the supramolecular chirality on each complex. However, the compound crystallized in a *P*-1 space group, so both $\Delta\Delta\Delta$ and $\Lambda\Lambda\Lambda$ enantiomers exist in the same crystal. The intramolecular distance between adjacent centroids of the triazine rings is determined to be 3.35 Å (Figure 1F), indicating the existence of strong intra-molecular π - π stacking interactions.^[14] As shown in the asymmetric unit in Figure 1G, two unique $\text{Eu}_3(\text{L4})_3$ assemblies with the same chirality are also closely packed together, giving rise to a dimeric structure, which is stabilized by multiple hydrogen-bonding interactions through three bridging OTf^- anions. Similarly, strong inter-molecular π - π stacking interactions are observed between the triphenyl-triazine plane, leading to a sextuple π - π stacked structure in total. The dimeric structures could also be found in the gas-phase, as assignable peaks corresponding to $[\text{Eu}_6(\text{L4})_6(\text{OTf})_{18-y}]^{y+}$ ($y=5,6,7$) were also observed in the ESI-TOF-MS (Figure 1D).

Complexes of $\text{Eu}_3(\text{L3})_3(\text{OTf})_9$ and $\text{Eu}_4(\text{L3})_4(\text{OTf})_{12}$. The $\text{Eu}_3(\text{L3})_3$ complex was synthesized in the same method as for $\text{Eu}_3(\text{L4})_3$ by using the corresponding **L3** and Eu^{III} salts. Due to the co-existence of potential $\Delta\Delta\Delta$, $\Delta\Delta\Lambda$, $\Delta\Lambda\Lambda$ and $\Lambda\Lambda\Lambda$ isomers,^[23] it is difficult to fully assign the ^1H NMR spectrum of this complex in this case (Figure 2A). Nonetheless, DOSY (Figure 2B) and ESI-TOF-MS (Figure 2G) clearly confirmed the formation of the trinuclear $\text{Eu}_3(\text{L3})_3(\text{OTf})_9$ structures in solution. Interestingly, when Eu^{III} and **L3** were self-assembled in nitromethane with a lower polarity, the $\text{Eu}_4(\text{L3})_4$ tetrahedral complex was obtained. This was firstly indicated by a totally different ^1H NMR spectrum (Figure 2C) from the $\text{Eu}_3(\text{L3})_3$ complex. Secondly, DOSY (Figure 2D) also indicated the formation of a single species with a different size (diffusion coefficient of $D = 3.98 \times 10^{-10} \text{ m}^2\text{s}^{-1}$ for $\text{Eu}_4(\text{L3})_4$), corresponding to a diameter of 16.8 Å), which is similar to the Eu_4L_4 -type complexes

reported previously.^[19] In addition, ESI-TOF-MS clearly confirmed the formation of $\text{Eu}_4(\text{L3})_4(\text{OTf})_{12}$, which showed a clear sequence of cationic peaks arising from the consecutive loss of OTf anions from the tetranuclear assembly (such as m/z 448.5025 ($[\text{Eu}_4(\text{L3})_4(\text{OTf})_1]^{8+}$), 533.7087 ($[\text{Eu}_4(\text{L3})_4(\text{OTf})_2]^{7+}$), 647.6517 ($[\text{Eu}_4(\text{L3})_4(\text{OTf})_3]^{6+}$), 806.9720 ($[\text{Eu}_4(\text{L3})_4(\text{OTf})_4]^{5+}$), 1045.7027 ($[\text{Eu}_4(\text{L3})_4(\text{OTf})_5]^{4+}$), 1444.2554 ($[\text{Eu}_4(\text{L3})_4(\text{OTf})_6]^{3+}$) (Figure 2H).

Attempts to crystallize $\text{Eu}_3(\text{L3})_3(\text{OTf})_9$ sandwich and $\text{Eu}_4(\text{L3})_4(\text{OTf})_{12}$ tetrahedron were unsuccessful possibly due to the existence of complicated isomers. Thus, their structures were simulated by molecular mechanic modeling. The optimized structure of $\Delta\Delta\Delta\text{-Eu}_3(\text{L3})_3$ and $\Delta\Delta\Delta\Delta\text{-Eu}_4(\text{L3})_4$ are shown in Figure 2E and 2F, respectively. The average distance of $\text{Eu}\cdots\text{Eu}$ of the $\Delta\Delta\Delta\text{-Eu}_3(\text{L3})_3$ are similar to $\text{Eu}_3(\text{L4})_3$. For $\text{Eu}_4(\text{L3})_4$, it is worth to mention that there are 25 possible isomeric structures by the combination of chirality at metal centers (Δ/Λ) and clockwise or anticlockwise orientation of ligands (A/C).^[24] (Table S2) Solvent-triggered transformation between $\text{Eu}_3(\text{L3})_3$ and $\text{Eu}_4(\text{L3})_4$ was then studied. When the nitromethane solution of $\text{Eu}_4(\text{L3})_4$ was evaporated and re-dissolved in acetonitrile by heating at 60°C for 1.5 h, both ^1H NMR (Figure S24) and ESI-TOF-MS (Figures S25, S47) spectra confirmed that structural transformation occurred. $\text{Eu}_3(\text{L3})_3$ could also be converted into $\text{Eu}_4(\text{L3})_4$ by solvent-exchange, and vice versa (Figures S22-S23, S48-S49). The successful transformation between the two complexes suggests the dynamic nature of these lanthanide-organic assemblies.

Photophysical studies. The UV-Vis absorption and photoluminescent properties of both ligands and complexes were investigated. Similar to the reported ligands, both **L3** and **L4** in CH_3CN solution show strong absorptions in the 235–320 nm range, respectively (Figure 3A). Upon excitation at 298 nm in the ligand level, $\text{Eu}_3(\text{L4})_3$ displays characteristic line-like emission peaks at 580, 593, 615, 650 and 702 nm, corresponding to $^5\text{D}_0 \rightarrow ^7\text{F}_J$ ($J = 0-4$) transitions of Eu^{III} (Figure 3B). However, sensitization performance of **L4** and **L3** were apparently different, with photoluminescent quantum yields Φ of $\text{Eu}_3(\text{L4})_3$ and $\text{Eu}_3(\text{L3})_3$ measured to be 55.3% and 34.7% in acetonitrile solution, respectively (Figure S28, S29). This is a little different from the previous report of Eu_4L_4 built from **L1** and **L2** with different

chelates connection angle, where analogous Φ (56% vs. 52%) were obtained.^[19] Similar characteristic Eu^{III} emission bands were also observed for $\text{Eu}_4(\text{L3})_4$, but the excitation band shows a little blue shifting. Under the same measurement conditions (0.3v% $\text{MeNO}_2/\text{MeCN}$), a smaller quantum yield ($\Phi=15.7\%$) was measured for $\text{Eu}_4(\text{L3})_4$ than $\text{Eu}_3(\text{L3})_3$ ($\Phi=23.2\%$). (See experimental section for details) This implies that the unique π - π stacked conformation of the ligands on the sandwich complexes dramatically enhanced the sensitization ability toward lanthanide luminescence. In our previous study, we have demonstrated that intra-ligand charge-transfer state provides a good alternative sensitization pathway toward bright luminescent cages.^[2c] The strong inter-ligand π - π stacking interactions observed on the triple-decker Ln_3L_3 sandwich motivated us to further modulate its luminescence based on a mixed ligands strategy.

Nonlinear enhanced luminescence on $\text{Eu}_3(\text{L3})_x(\text{L4})_{3-x}$. Luminescence modulation by doping of different organic ligands has been studied in MOFs and other nanomaterials.^[25] However, such a doping has seldom been tested on the molecular level.^[26] We designed the following experiments to confirm that intra-ligand charge-transfer state can be used to enhance the luminescence of the lanthanide-organic edifices. Firstly, when equimolar amount of $\text{Eu}(\text{OTf})_3$ and mixed **L4/L3** (2:1 molar ratio) was self-assembled, formation of heteroligand $\text{Eu}_3(\text{L4})_x(\text{L3})_{3-x}$ ($x = 0, 1, 2, 3$) sandwiches was confirmed by ESI-TOF-MS (Figure S35). The emission spectra ($\lambda_{\text{ex}} = 298$ nm) were collected with the gradually increased fraction of the **L4** content [$f = \text{L4}/(\text{L3}+\text{L4})$]. As shown in Figure 3C, the emission intensity at 615 nm shows a nonlinear enhancing trend with two maxima appeared at $f = 0.4$ and 0.7, respectively. These are the ratios where $\text{Eu}_3(\text{L4})_1(\text{L3})_2$ or $\text{Eu}_3(\text{L4})_2(\text{L3})_1$ are preferably formed (Figures S51-S54). As a control, the emission intensity (615 nm) shows a linear change by systematically mixing of the preformed $\text{Eu}_3(\text{L3})_3$ and $\text{Eu}_3(\text{L4})_3$ complexes (Figure S54-S59). We speculate that the formation of A-D-A or D-A-D type π - π stackings between the triphenylbenzene (Donor, D) and triphenyltriazine (Acceptor, A) aromatic panels on the ligands accounts for the bactrian-shape of the emission enhancement. This was further supported by the UV-vis spectrum, where heteroligand complexes of $\text{Eu}_3(\text{L4})_x(\text{L3})_{3-x}$ ($x = 1$ and 2) showed slightly enhanced absorption at 300 nm compared to the

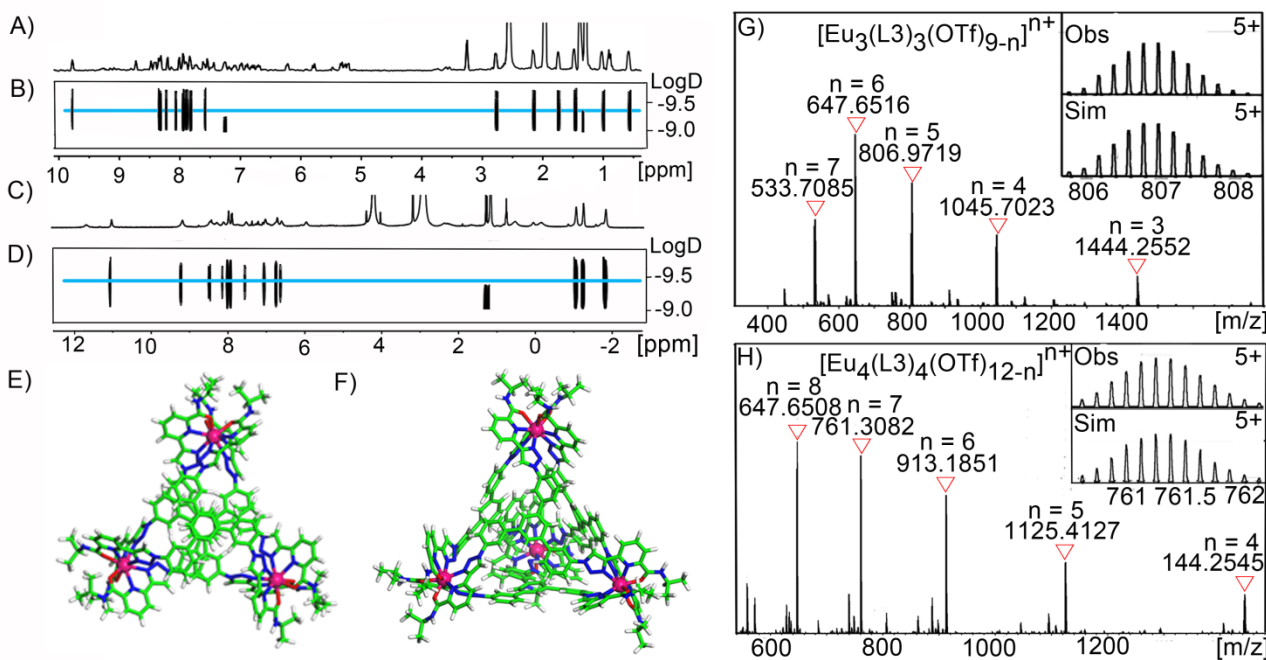
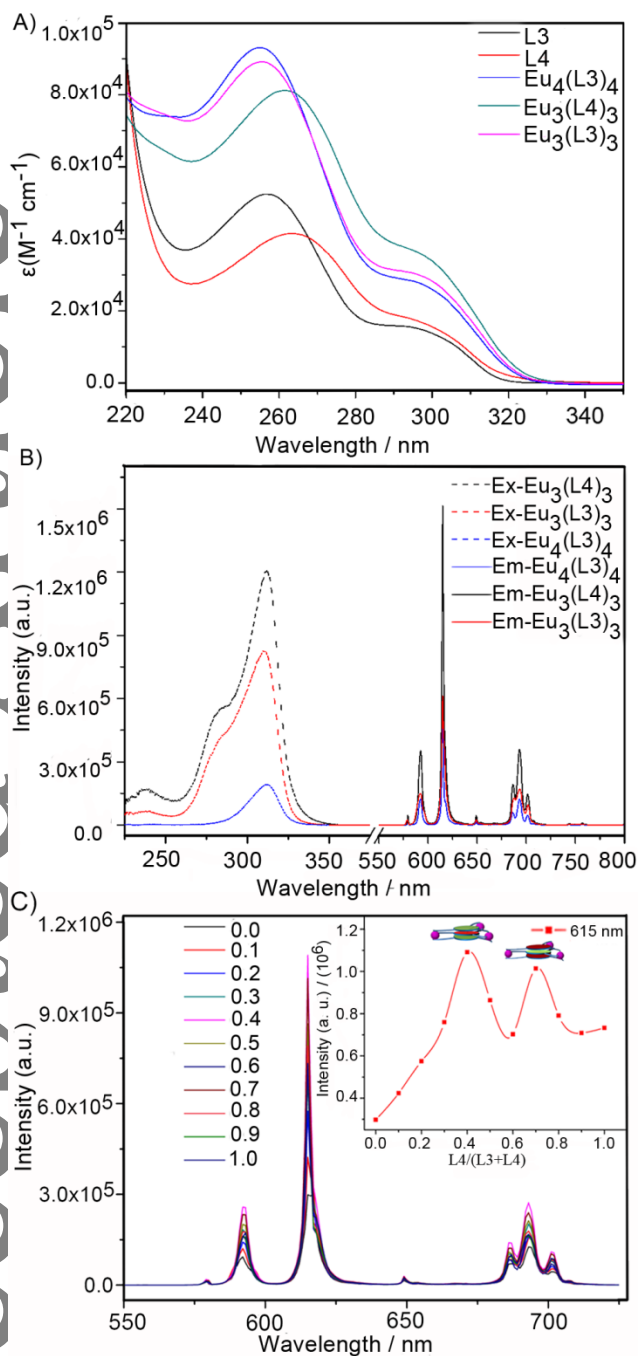


Figure 2 Self-assembly of **L3** with $\text{Eu}(\text{OTf})_3$. ^1H NMR (400 MHz, 293 K) spectra of (A) the $\text{Eu}_3(\text{L3})_3(\text{OTf})_9$ complexes (in $\text{CD}_3\text{CN}/\text{CD}_3\text{OD}$) and (C) the $\text{Eu}_4(\text{L3})_4(\text{OTf})_{12}$ complexes (in $\text{CD}_3\text{NO}_2/\text{CD}_3\text{OD}$); ^1H DOSY spectra of (B) the $\text{Eu}_3(\text{L3})_3(\text{OTf})_9$ complexes and (D) the $\text{Eu}_4(\text{L3})_4(\text{OTf})_{12}$ complexes; Energy minimized structure of (E) $\text{Eu}_3(\text{L3})_3$ and (F) $\text{Eu}_4(\text{L3})_4$. ESI-TOF-MS spectra of (G) the $\text{Eu}_3(\text{L3})_3$ and (H) the $\text{Eu}_4(\text{L3})_4$, with insets showing the observed and simulated isotopic patterns of the peaks corresponding to $[\text{Eu}_3(\text{L3})_3(\text{OTf})_4]^{5+}$ and $[\text{Eu}_4(\text{L3})_4(\text{OTf})_7]^{5+}$, respectively. For clarity, only the tetrahedral framework is shown. Eu, purple sphere; C, green; N, dark blue; O, red; H, white.

mix-complex solutions ($\text{Eu}_3(\text{L3})_3/\text{Eu}_3(\text{L4})_3=1/2$ or $2/1$) (Figure S33). **Figure 3** (A) UV-Vis absorption of **L3**, **L4** and $\text{Eu}_3(\text{L4})_3$, $\text{Eu}_3(\text{L3})_3$ and $\text{Eu}_4(\text{L3})_4$



in CH_3CN ($c = 1 \times 10^{-5}$ M) (B) Excitation and emission of $\text{Eu}_3(\text{L4})_3$, $\text{Eu}_3(\text{L3})_3$ and $\text{Eu}_4(\text{L3})_4$ in CH_3CN ($c = 1 \times 10^{-5}$ M). (C) The emission spectra (CH_3CN , $c = 1 \times 10^{-5}$ M, $\lambda_{\text{ex}} = 298$ nm) of the mixed-ligand $\text{Eu}_3(\text{L4})_x(\text{L3})_{3-x}$ ($x = 0-3$) complexes with increasing content of **L4** [$f = \text{L4}/(\text{L3}+\text{L4})$] (Inset shows the changes of the emission intensity at 615 nm at different f values with two schematic diagrams of the dominate species of $\text{Eu}_3(\text{L4})_1(\text{L3})_2$ and $\text{Eu}_3(\text{L4})_2(\text{L3})_1$ at $f = 0.4$ and 0.7 , respectively).

Conclusions

Unprecedented supramolecular lanthanide-organic sandwich complexes were obtained by a small variation of ligand conformations, and the first example of sandwich-to-tetrahedron transformation was observed based on solvent effect. Moreover, nonlinear enhancement of lanthanide luminescence based on the modulation of inter-ligand charge-transfer state has been realized.

Our results provide important guidance for structure-design and photoluminescence optimization of supramolecular lanthanide-organic assemblies.

Experimental

Materials and Methods. Unless otherwise stated, all chemicals and solvents were purchased from commercial companies and used without further purification. Anhydrous solvents were distilled according to standard procedures. The solvents used for photophysical measurements were of HPLC grade. Deuterated solvents were purchased from Admas, J&K scientific and Sigma-Aldrich. 1D and 2D-NMR spectra were measured on a Bruker Biospin Avance III (400 MHz) spectrometer. ^1H -NMR chemical shifts were determined with tetramethylsilane (TMS) or respect to residual signals of the deuterated solvents used. ESI-TOF-MS mass spectra were recorded on Impact II UHR-TOF from Bruker, with tuning mix as the internal calibrant. Data analysis was conducted with the Bruker Data Analysis software (Version 4.3) and simulations were performed with the Bruker Isotope Pattern software. UV-Vis spectra were recorded on UV-2700 spectrometer from SHIMADZU. Excitation and emission spectra were recorded on F55 and FLSP920 spectrofluorometer from Edinburg Photonics. Spectra were corrected for the experimental functions. The emission quantum yields in solution and solid state were measured by F55 spectrofluorometer from Edinburg Photonics with integrating sphere.

$\text{Eu}_3(\text{L4})_3(\text{OTf})_9$: To a suspension of ligand **L4** (3.03 mg, 3.03×10^{-3} mmol, 1 equiv) and $\text{Eu}(\text{OTf})_3$ (2.19 mg, 3.16×10^{-3} mmol, 1.1 equiv) in 1 mL MeCN at 25°C for 1 h, the turbid suspension of ligands gradually turned clear. The solid progressively dissolved to give a resulting homogeneous yellow solution. ^1H NMR showed the quantitative formation of $\text{Eu}_3(\text{L4})_3(\text{OTf})_9$, m.p. $>300^\circ\text{C}$. ^1H NMR (CD_3CN , 400 MHz) δ 9.91 (s, 1H), 8.46 (d, $J = 11.4$ Hz, 2H), 8.39 (s, 1H), 8.24 (d, $J = 7.8$ Hz, 1H), 7.88 (d, $J = 7.1$ Hz, 1H), 7.65 (s, 1H), 7.56 (d, $J = 6.2$ Hz, 1H), 7.47 (d, $J = 7.8$ Hz, 1H), 7.37 (dd, $J = 12.9$, 7.4 Hz, 2H), 7.25 (t, $J = 7.4$ Hz, 1H), 7.10 (s, 2H), 7.01 (t, $J = 8.1$ Hz, 1H), 6.92 (d, $J = 7.9$ Hz, 2H), 6.61 (t, $J = 7.6$ Hz, 1H), 6.29 (d, $J = 7.3$ Hz, 1H), 6.19 (t, $J = 7.8$ Hz, 1H), 5.78 (s, 1H), 5.36 (d, $J = 7.1$ Hz, 1H), 5.17 (d, $J = 7.1$ Hz, 1H), 4.83 (d, $J = 7.5$ Hz, 1H), 4.50 (d, $J = 7.8$ Hz, 1H), 4.03 (s, 1H), 3.66 (s, 1H), 3.23 (s, 1H), 2.21 (s, 3H), 1.27 (dd, $J = 10.5$, 5.4 Hz, 6H), 1.10 (d, $J = 4.9$ Hz, 3H), 0.29 (dd, $J = 12.7$, 5.5 Hz, 6H). HRMS for $\text{Eu}_3(\text{L4})_3(\text{OTf})_9$: The following picked signals are those at the high intensities. m/z calcd for $[\text{M}-3(\text{CF}_3\text{SO}_3^-)]^{3+}$ 1447.2414, found 1447.2412; calcd for $[\text{M}-4(\text{CF}_3\text{SO}_3^-)]^{4+}$ 1047.9427, found 1047.9420; calcd for $[\text{M}-5(\text{CF}_3\text{SO}_3^-)]^{5+}$ 808.5637, found 808.5632; calcd for $[\text{M}-6(\text{CF}_3\text{SO}_3^-)]^{6+}$ 649.1445, found 649.1445; calcd for $[\text{M}-7(\text{CF}_3\text{SO}_3^-)]^{7+}$ 534.9877, found 534.9883.

$\text{Eu}_3(\text{L3})_3(\text{OTf})_9$: $\text{Eu}_3(\text{L3})_3(\text{OTf})_9$ was prepared by a same procedure as $\text{Eu}_3(\text{L4})_3(\text{OTf})_9$. m.p. $>300^\circ\text{C}$. ^1H NMR ($\text{CD}_3\text{CN}/\text{CD}_3\text{OD}$ $v/v = 4:1$, 400 MHz, 298 K) δ 9.78 (s, 2H), 8.73 (s, 1H), 8.48 (s, 1H), 8.41 (d, $J = 7.9$ Hz, 1H), 8.20 (s, 1H), 8.01 (s, 1H), 7.94 (d, $J = 5.5$ Hz, 1H), 7.91 (d, $J = 10.2$ Hz, 2H), 7.83 (d, $J = 5.3$ Hz, 2H), 7.75 (d, $J = 8.8$ Hz, 1H), 7.60 (d, $J = 10.2$ Hz, 1H), 7.55 (s, 1H), 7.46 (dd, $J = 15.0$, 5.9 Hz, 2H), 7.26 (t, $J = 6.7$ Hz, 2H), 7.19 (d, $J = 9.1$ Hz, 1H), 7.13 – 7.07 (m, 1H), 6.99 (d, $J = 7.2$ Hz, 1H), 6.90 (d, $J = 8.1$ Hz, 1H), 6.80 (t, $J = 6.4$ Hz, 1H), 6.73 – 6.67 (m, 1H), 6.59 (d, $J = 12.4$ Hz, 1H), 6.25 – 6.14 (m, 2H), 5.79 (d, $J = 7.2$ Hz, 1H), 5.35 – 5.22 (m, 3H), 3.57 (d, $J = 16.2$ Hz, 1H), 2.78 (d, $J = 5.6$ Hz, 3H), 2.16 (d, $J = 5.7$ Hz, 3H), 1.74 (d, $J = 5.9$ Hz, 3H), 1.48 (d, $J = 5.5$ Hz, 3H), 1.03 (d, $J = 6.1$ Hz, 3H), 0.58 (d, $J = 5.6$ Hz, 3H); HRMS for $\text{Eu}_3(\text{L3})_3(\text{OTf})_9$: The following picked signals are those at the highest intensities. m/z calcd for $[\text{M}-3(\text{CF}_3\text{SO}_3^-)]^{3+}$ 1444.2558, found 1444.2544; calcd for $[\text{M}-4(\text{CF}_3\text{SO}_3^-)]^{4+}$ 1045.7019, found 1045.7035; calcd for $[\text{M}-5(\text{CF}_3\text{SO}_3^-)]^{5+}$ 806.7713, found 806.7723; calcd for $[\text{M}-6(\text{CF}_3\text{SO}_3^-)]^{6+}$ 647.6513, found 647.6517; calcd for $[\text{M}-$

$7(\text{CF}_3\text{SO}_3^-)^{7+}$ 533.7084, found 533.7081.

Eu₄(L3)₄(OTf)₁₂: To a suspension of ligand **L3** (4.01 mg, 4.02×10^{-3} mmol, 1 equiv.) and Eu(OTf)₃ (2.89 mg, 4.83×10^{-3} mmol, 1.2 equiv) in 1 mL MeNO₂ at 50°C for 1.5 h, the turbid suspension of ligands gradually turned clear. The solid progressively dissolved to give a resulting homogeneous yellow solution. ¹H NMR showed the quantitative formation of Eu₄(L3)₄(OTf)₁₂. However, its NMR spectra could not be assigned due to the poor solubility of this complex. m.p. >300 °C. HRMS for Eu₄(L3)₄(OTf)₁₂: The following picked signals are those at the high intensities. *m/z* calcd for [M-4(CF₃SO₃⁻)]⁴⁺ 1444.2558, found 1444.2545; calcd for [M-5(CF₃SO₃⁻)]⁵⁺ 1125.4139, found 1125.4129; calcd for [M-6(CF₃SO₃⁻)]⁶⁺ 913.1864, found 913.1853; calcd for [M-7(CF₃SO₃⁻)]⁷⁺ 761.3093, found 761.3083; calcd for [M-8(CF₃SO₃⁻)]⁸⁺ 647.6517, found 647.6509; [M-9(CF₃SO₃⁻)]⁹⁺ 559.0289, found 559.0286; calcd for [M-10(CF₃SO₃⁻)]¹⁰⁺ 488.2308, found 488.2311.

Supporting Information

The supporting information for this article is available on the WWW under <https://doi.org/10.1002/cjoc.2018xxxxx>.

Acknowledgement (optional)

This work was supported by the NSFC (Grant Nos. 21825107, 21601183, 2017J05037), the Strategic Priority Research Program of the Chinese Academy of Sciences (Grant No. XDB20000000).

References

- [1] (a) Fiedler, D.; Leung, D.H.; Bergman, R.G.; Raymond, K.N. Selective Molecular Recognition, C–H Bond Activation, and Catalysis in Nanoscale Reaction Vessels, *Acc. Chem. Res.* **2005**, *38*, 349–358; (b) Wiester, M.J.; Ulmann, P.A.; Mirkin, C.A. Enzyme mimics based upon supramolecular coordination chemistry, *Angew. Chem. Int. Ed.* **2011**, *50*, 114–137.
- [2] (a) Liu, C.L.; Zhou, L.P.; Tripathy, D.; Sun, Q.F. Self-assembly of stable luminescent lanthanide supramolecular M₄L₆ cages with sensing properties toward nitroaromatics, *Chem. Commun.* **2017**, *53*, 2459–2462; (b) Zhang, K.; Xie, X.; Li, H.; Gao, J.; Nie, L.; Pan, Y.; Xie, J.; Tian, D.; Liu, W.; Fan, Q.; Su, H.; Huang, L.; Huang, W. Highly Water-Stable Lanthanide–Oxalate MOFs with Remarkable Proton Conductivity and Tunable Luminescence, *Adv. Mater.* **2017**, *29*, 1701804; (c) Liu, C.L.; Zhang, R.L.; Lin, C.S.; Zhou, L.P.; Cai, L.X.; Kong, J.T.; Yang, S.Q.; Han, K.L.; Sun, Q.F. Intraligand Charge Transfer Sensitization on Self-Assembled Europium Tetrahedral Cage Leads to Dual-Selective Luminescent Sensing toward Anion and Cation, *J. Am. Chem. Soc.* **2017**, *139*, 12474–12479.
- [3] Li, X.Z.; Zhou, L.P.; Yan, L.L.; Dong, Y.M.; Bai, Z.L.; Sun, X.Q.; Diwu, J.; Wang, S.; Bunzli, J.C.; Sun, Q.F. A supramolecular lanthanide separation approach based on multivalent cooperative enhancement of metal ion selectivity, *Nat. Commun.* **2018**, *9*, 547–556.
- [4] (a) Bunzli, J.C. Lanthanide luminescence for biomedical analyses and imaging, *Chem. Rev.* **2010**, *110*, 2729–2755; (b) Zhou, Z.; Liu, J.; Rees, T.W.; Wang, H.; Li, X.; Chao, H.; Stang, P.J. Heterometallic Ru–Pt metallacycle for two-photon photodynamic therapy, *PNAS.* **2018**, *115*, 5664–5669; (c) Stang, P.J.; Olenyuk, B. Self-Assembly, Symmetry, and Molecular Architecture: Coordination as the Motif in the Rational Design of Supramolecular Metallacyclic Polygons and Polyhedra, *Acc. Chem. Res.* **1997**, *30*, 502–518.
- [5] (a) Caulder, D.L.; Raymond, K.N. Supermolecules by Design, *Acc. Chem. Res.* **1999**, *32*, 975–982; (b) Chakrabarty, R.; Mukherjee, P.S.; Stang, P.J. Supramolecular coordination: self-assembly of finite two- and three-dimensional ensembles, *Chem. Rev.* **2011**, *111*, 6810–6918; (c) Cook, T.R.; Stang, P.J. Recent Developments in the Preparation and Chemistry of Metallacycles and Metallacages via Coordination, *Chem. Rev.* **2015**, *115*, 7001–7045; (d) Fujita, M.; Tominaga, M.; Hori, A.; Therrien, B. Coordination assemblies from a Pd(II)-cornered square complex, *Acc. Chem. Res.* **2005**, *38*, 369–378; (e) Yoshizawa, M.; Klosterman, J.K.; Fujita, M. Functional molecular flasks: new properties and reactions within discrete, self-assembled hosts, *Angew. Chem. Int. Ed.* **2009**, *48*, 3418–3438; (f) Holliday, B.J.; Mirkin, C.A. Strategies for the Construction of Supramolecular Compounds through Coordination Chemistry, *Angew. Chem. Int. Ed.* **2001**, *40*, 2022–2043; (g) Smulders, M.M.; Riddell, I.A.; Browne, C.; Nitschke, J.R. Building on architectural principles for three-dimensional metallosupramolecular construction, *Chem. Soc. Rev.* **2013**, *42*, 1728–1754; (h) Chen, L.; Chen, Q.; Wu, M.; Jiang, F.; Hong, M. Controllable coordination-driven self-assembly: from discrete metallocages to infinite cage-based frameworks, *Acc. Chem. Res.* **2015**, *48*, 201–210.
- [6] (a) Li, X.Z.; Zhou, L.P.; Yan, L.L.; Yuan, D.Q.; Lin, C.S.; Sun, Q.F. Evolution of Luminescent Supramolecular Lanthanide M₂nL₃n Complexes from Helicates and Tetrahedra to Cubes, *J. Am. Chem. Soc.* **2017**, *139*, 8237–8244; (b) Jing, X.; He, C.; Yang, Y.; Duan, C. A metal-organic tetrahedron as a redox vehicle to encapsulate organic dyes for photocatalytic proton reduction, *J. Am. Chem. Soc.* **2015**, *137*, 3967–3974; (c) Hamacek, J.; Poggiali, D.; Zebret, S.; El Aroussi, B.; Schneider, M.W.; Mastalerz, M. Building large supramolecular nanocapsules with europium cations, *Chem. Commun.* **2012**, *48*, 1281–1283.
- [7] (a) Bunzli, J.-C.G.; Piguet, C. Lanthanide-Containing Molecular and Supramolecular Polymetallic Functional Assemblies, *Chem. Rev.* **2002**, *102*, 1897–1928; (b) Butler, S.J.; Parker, D. Anion binding in water at lanthanide centres: from structure and selectivity to signalling and sensing, *Chem. Soc. Rev.* **2013**, *42*, 1652–1666; (c) Barry, D.E.; Caffrey, D.F.; Gunnlaugsson, T. Lanthanide-directed synthesis of luminescent self-assembly supramolecular structures and mechanically bonded systems from acyclic coordinating organic ligands, *Chem. Soc. Rev.* **2016**, *45*, 3244–3274; (d) Sabbatini, N.; Guardigli, M.; Lehn, J.M. Luminescent Lanthanide Complexes as Photochemical Supramolecular Devices, *Coordin. Chem. Rev.* **1993**, *123*, 201–228.
- [8] El Aroussi, B.; Zebret, S.; Besnard, C.; Perrotet, P.; Hamacek, J. Rational design of a ternary supramolecular system: self-assembly of pentanuclear lanthanide helicates, *J. Am. Chem. Soc.* **2011**, *133*, 10764–10767.
- [9] Wang, W.; Wang, Y.X.; Yang, H.B. Supramolecular transformations within discrete coordination-driven supramolecular architectures, *Chem. Soc. Rev.* **2016**, *45*, 2656–2693.
- [10] Zarra, S.; Clegg, J.K.; Nitschke, J.R. Selective assembly and disassembly of a water-soluble Fe₁₀L₁₅ prism, *Angew. Chem. Int. Ed.* **2013**, *52*, 4837–4840.
- [11] Stephenson, A.; Argent, S.P.; Riis-Johannessen, T.; Tidmarsh, I.S.; Ward, M.D. Structures and dynamic behavior of large polyhedral coordination cages: an unusual cage-to-cage interconversion, *J. Am. Chem. Soc.* **2011**, *133*, 858–870.
- [12] Lusby, P.J.; Muller, P.; Pike, S.J.; Slawin, A.M. Stimuli-responsive reversible assembly of 2D and 3D metallosupramolecular architectures, *J. Am. Chem. Soc.* **2009**, *131*, 16398–16400.
- [13] Han, M.; Michel, R.; He, B.; Chen, Y.S.; Stalke, D.; John, M.; Clever, G.H. Light-triggered guest uptake and release by a photochromic coordination cage, *Angew. Chem. Int. Ed.* **2013**, *52*, 1319–1323.
- [14] Sorensen, A.; Castilla, A.M.; Ronson, T.K.; Pittelkow, M.; Nitschke, J.R. Chemical signals turn on guest binding through structural reconfiguration of triangular helicates, *Angew. Chem. Int. Ed.* **2013**, *52*, 11273–11277.
- [15] Scherer, M.; Caulder, D.L.; Johnson, D.W.; Raymond, K.N. Triple Helicate–Tetrahedral Cluster Interconversion Controlled by Host–Guest Interactions, *Angew. Chem. Int. Ed.* **1999**, *38*, 1587–1592.
- [16] Georges, J. Lanthanide-sensitized luminescence and applications to the determination of organic analytes. A review, *Analyst.* **1993**, *118*, 1481–1486.
- [17] Ma, Y.; Wang, Y. Recent advances in the sensitized luminescence of organic europium complexes, *Coordin. Chem. Rev.* **2010**, *254*, 972–990.
- [18] (a) Bunzli, J.-C.G. On the design of highly luminescent lanthanide complexes, *Coordin. Chem. Rev.* **2015**, *293–294*, 19–47; (b) Amoroso, A.J.; Pope, S.J. Using lanthanide ions in molecular bioimaging, *Chem. Soc. Rev.* **2015**, *44*, 4723–4742.
- [19] Guo, X.Q.; Zhou, L.P.; Cai, L.X.; Sun, Q.F. Self-assembled bright luminescent lanthanide-organic polyhedra for ratiometric temperature

sensing, *Chem. Eur. J.* **2018**, *24*, 6936-6940.

[20] (a) Hamacek, J.; Bernardinelli, G.; Filinchuk, Y. Tetrahedral assembly with lanthanides: Toward discrete polynuclear complexes, *Eur. J. Inorg. Chem.* **2008**, *2008*, 3419-3422; (b) Yan, L.L.; Tan, C.H.; Zhang, G.L.; Zhou, L.P.; Bunzli, J.C.; Sun, Q.F. Stereocontrolled self-assembly and self-sorting of luminescent Europium tetrahedral cages, *J. Am. Chem. Soc.* **2015**, *137*, 8550-8555.

[21] Caulder, D.L.; Powers, R.E.; Parac, T.N.; Raymond, K.N. The Self-Assembly of a Pre-designed Tetrahedral M_4L_6 Supramolecular Cluster, *Angew. Chem. Int. Ed.* **1998**, *37*, 1840-1843.

[22] Spek, A.L. Single-crystal structure validation with the program PLATON, *J. Appl. Crystallogr.* **2003**, *36*, 7-13.

[23] Hong, C.M.; Kaphan, D.M.; Bergman, R.G.; Raymond, K.N.; Toste, F.D. Conformational Selection as the Mechanism of Guest Binding in a Flexible Supramolecular Host, *J. Am. Chem. Soc.* **2017**, *139*, 8013-8021.

[24] Qu, H.; Tang, X.; Wang, X.; Li, Z.; Huang, Z.; Zhang, H.; Tian, Z.; Cao, X. Chiral molecular face-rotating sandwich structures constructed through restricting the phenyl flipping of tetraphenylethylene, *Chem. Sci.* **2018**, *9*, 8814-8818.

[25] (a) Chen, C.X.; Qiu, Q.F.; Pan, M.; Cao, C.C.; Zhu, N.X.; Wang, H.P.; Jiang, J.J.; Wei, Z.W.; Su, C.Y. Tunability of fluorescent metal-organic frameworks through dynamic spacer installation with multivariate fluorophores, *Chem. Commun.* **2018**, *54*, 13666-13669; (b) Zhang, X.; Wang, W.; Hu, Z.; Wang, G.; Uvdal, K. Coordination polymers for energy transfer: Preparations, properties, sensing applications, and perspectives, *Coordin. Chem. Rev.* **2015**, *284*, 206-235.

[26] (a) Yuasa, J.; Ohno, T.; Miyata, K.; Tsumatori, H.; Hasegawa, Y.; Kawai, T. Noncovalent ligand-to-ligand interactions alter sense of optical chirality in luminescent tris(beta-diketonate) lanthanide(III) complexes containing a chiral bis(oxazolonyl) pyridine ligand, *J. Am. Chem. Soc.* **2011**, *133*, 9892-9902; (b) Koizuka, T.; Yanagisawa, K.; Hirai, Y.; Kitagawa, Y.; Nakanishi, T.; Fushimi, K.; Hasegawa, Y. Red luminescent Eu(III) coordination bricks excited on blue LED chip, *Inorg. Chem.* **2018**, *57*, 7097-7103.

(The following will be filled in by the editorial staff)

Manuscript received: XXXX, 2019

Manuscript revised: XXXX, 2019

Manuscript accepted: XXXX, 2019

Accepted manuscript online: XXXX, 2019

Version of record online: XXXX, 2019

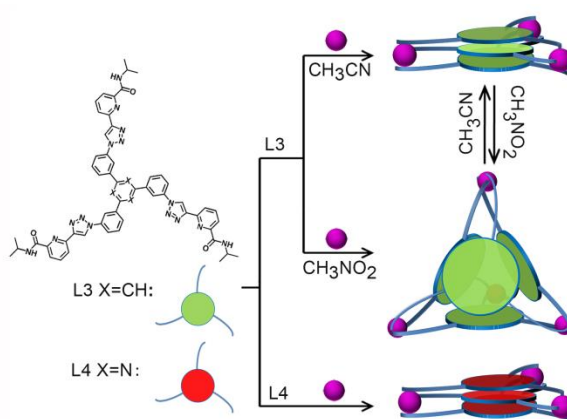
Entry for the Table of Contents

Page No.

Title

Coordination-Assembled Lanthanide-Organic
 Ln_3L_3 Sandwiches or Ln_4L_4 Tetrahedron:
 Structural Transformation and Luminescence
 Modulation

Shao-Jun Hu, Xiao-Qing Guo, Li-Peng Zhou,
 Li-Xuan Cai and Qing-Fu Sun*



^a State Key Laboratory of Structural Chemistry, Fujian Institute of Research on the Structure of Matter, Chinese Academy of Sciences, Fuzhou 350002, PR China
 E-mail:

^c University of Chinese Academy of Sciences, Beijing 100049, PR China
 E-mail:

^b College of Chemistry, Fuzhou University, Fuzhou 350108, PR China
 E-mail: